Journal of Superconductivity and Novel Magnetism (2020) 33:965–970
https://doi.org/10.1007/s10948-019-05336-w

ORIGINAL PAPER

The Influence of Nano-Sized SnO_2 Doping on Physical and Magnetic Properties of the $Bi_2Sr_{2-x}(SnO_2)_xCa_1Cu_{1.75}Na_{0.25}O_y$ Superconductors

Mehmet Ersin Aytekin[1] · Berdan Özkurt[2]

Received: 24 August 2019 / Accepted: 4 October 2019 / Published online: 24 November 2019

Abstract

In this study, we have investigated the effect of nano-sized SnO_2 (50 nm) doping on the superconducting properties of Bi-2212 ceramics. In the first stage of the the experiment, the composition $Bi_2Sr_{2-x}Sn_xCa_1Cu_{1.75}Na_{0.25}O_y$ where $x = 0$, 0.05, 0.1 and 0.2 is selected due to the positive effect of sodium substitution on the grain sizes of the Bi-2212. X-ray diffraction results indicate that all the samples have considerable amount of Bi-2212 phases. Scanning electron microscopy (SEM) analysis of all samples clearly shows significant grain growth due to lower crystallization temperature formed by sodium. The lowest resistivity in the nano-sized SnO_2-doped samples at 150 K is obtained for the sample of $x = 0.05$. The *M-H* hysteresis loops for all the samples have been measured within ± 2 T externally applied magnetic field range at $T = 15$ and 25 K, respectively. The undoped and the sample with $x = 0.05$ SnO_2 have both large *M-H* loops, indicating the improvement of flux pinning properties of the Bi-2212 as well as enhanced intergrain connectivity. However, the width of the hysteresis loop in samples including high ($x > 0.05$) SnO_2 contents significantly decreased, indicating deterioration in superconducting properties of the Bi-2212 system. Additionally, the critical current densities (J_c) of all the samples at 15 K are calculated from their hysteresis loop measurements by using Bean's critical state model. When compared with other samples, a slight increase in J_c is obtained for $x = 0.05$ SnO_2. The results indicate that the optimal contents of sodium ($x = 0.25$) and nano-sized SnO_2 ($x = 0.05$) in the Bi-2212 system are effective for achieving enhanced superconductivity properties.

Keywords $Bi_2Sr_{2-x}(SnO_2)_xCa_1Cu_{1.75}Na_{0.25}O_y$ · XRD · SEM · Magnetic hysteresis loop

1 Introduction

The discovery of BSCCO ceramics including different superconducting phases according to copper oxide numbers (n) in its crystal structure with the chemical formula $Bi_2Sr_2Ca_{n-1}Cu_nO_y$ has enabled the lossless transmission of the electricity, which is required for their use in technological applications such as high-powered devices, magnetic field engineering applications (maglev vehicle), and new electronic equipments [1–5].

Bi-2212 phase having transition temperature of about 90 K in the BSCCO system is highly stable, thermodynamically. This means that the substitution or addition of many useful elements such as Nb, B Cd, Sn, and Pb without the destruction of its phase formation can be done to improve its superconducting properties [6–11]. It is well known that the vortex region in all type II superconductors covers the range lying between H_{c1} and H_{c2} and the material can maintain superconductivity properties as long as the applied magnetic field remains below the values of H_{c2}. However, the H_{c2} (upper critical field) decreases very quickly at high temperatures, which prevents widespread use of superconductors. Nevertheless, it is also possible to increase H_{c2} values to higher values by preventing vortex movements which occur as a result of large currents passing through the material, thanks to the formation of natural or artificial effective pinning centers in the type II superconductors. On the other hand, the enhanced H_{c2} also reflects the increases in the critical current density values (J_c) of the type II superconductors. Furthermore, the enhancements of J_c in high-temperature superconductors strongly depend on the improvements in their weak flux pinning capabilities as well as more uniformly

✉ Berdan Özkurt
berdanozkurt@tarsus.edu.tr

[1] Advanced Technology Research and Application Center, Mersin University, Yenişehir, TR-33343 Mersin, Turkey

[2] Department of Energy Systems Engineering, Faculty of Technology, Tarsus University, 33400 Tarsus, Turkey

ordered grain orientations obtained by using the laser techniques such as laser floating zone (LFZ) and the electrically assisted laser floating zone (EALFZ) [12–16].

There are many studies in the literature showing the enhanced flux pinning by the addition or substitutions of nano-sized elements such as ZrO_2, SiC, MgO, and Al_2O_3 into the BSCCO system [17–20]. Another element on the nanoscale which has a significant effect on the J_c values of the BSCCO system is SnO_2, ensuring the enhancement in intergranular flux pinning when its appropriate content is especially selected [21–23].

It is obvious from the literature that the critical current density values in the Bi-based superconductors can be enhanced significantly by doping or adding of the alkali elements such as Na, Li, K, Rb, and Cs [1, 24–26]. Thus, $Bi_2Sr_2Ca_1Cu_{1.75}Na_{0.25}O_y$ was chosen as the initial composition in this work because of the positive effect of the Na element on grain sizes [1].

In the present study, the effect of nano-SnO_2 particles (50 nm) substitution to Bi-2212 superconducting phase in $Bi_2Sr_{2-x}(SnO_2)_xCa_1Cu_{1.75}Na_{0.25}O_y$ (x = 0.0, 0.05, 0.1, 0.20) composition has been investigated by XRD, SEM, DC resistivity, and magnetic hysteresis measurements. Finally, we examined the change of magnetic J_c values calculated from the M-H loops of samples by using Bean's critical state model.

2 Experimental Details

Ceramic superconductor samples with nominal composition $Bi_2Sr_{2-x}(SnO_2)_xCa_1Cu_{1.75}Na_{0.25}O_y$ (x = 0.0, 0.05, 0.1, 0.20) in this study were prepared by using the standard solid-state reaction methods with high purity initial powders Bi_2O_3 (Panreac, 98+%), $SrCO_3$ (Panreac, 98+%), $CaCO_3$ (Panreac, 98.5+%), CuO (Panreac, 97+%) and SnO_2 (ABO Switzerland Co., Ltd. 99+%).

For homogeneous mixing of precursor powders in the solid-state reaction, grinding processes such as agate mortars or ball mills were used. When these grinding methods are used, they may lead to loss of materials and may cause deterioration in the crystal structure due to the adhesion of the powders to the pot in the grinding process [27]. In this study, a combination of nitric acid and pure water was used to prevent such losses in the material.

The precursor powders with appropriate proportion were mixed in the magnetic stirrer until it was completely dissolved in the nitric acid solution. When a homogeneous solution was obtained, it turned into light blue. Then, the distilled water and nitric acid solution were evaporated to obtain black powder. To completely dry the powders, heat treatment was applied at around 350 °C. A homogeneous mixture of powders was pressed into pellets of 2.9-cm diameter by applying a 375 MPa pressure, and then calcined at 750 °C for 12 h in order to decompose the carbonates. The calcined pellets were reground, repressed, and recalcined at 820 °C for 12 h to reach the high phase-purity (2212 phase). These stages including milling, pressing, and calcining were repeated two times. Finally, precursor pellets were ground, repressed, and annealed at 850 °C for 120 h in order to reach a large amount of pure Bi-2212 phase.

Samples with x = 0, 0.05, 0.1, and 0.2 nano-sized SnO_2 contents will hereafter be named A, B, C, and D, respectively.

Resistivity and magnetic measurements were carried out on the samples using Cryogenic Limited PPMS (from 5 to 300 K) which can reach the cryogenic temperatures to about 2 K in a closed-loop He system. X-ray powder diffraction analyses to determine the phases present in the samples were performed by using a Rigaku Ultima IV X-Ray Diffractometer with a constant scan rate (2°/min) in the range $2\theta = 3°–60°$. Lattice parameters were automatically calculated by the PDXL software version 1.6.0.1 with the ICDD version 6.0 database. The surface morphologies of the samples were studied by using a Zeiss/Supra 55 scanning electron microscopy (SEM).

3 Results and Discussion

Figure 1 shows powder XRD patterns for all the samples. The main peaks in all samples are indexed as the Bi-2212 phase. Their peak intensities are also similar, meaning that the differences in crystallite sizes of samples can be negligible because the crystallite size calculated by the conventional Scherrer equation significantly depends on the changes in the diffraction peak widths which do not change effectively as seen in this study [28].

On the other hand, the lattice constants of all samples are given in Table 1. They have tetragonal crystal structure. In general, foreign ions added into the Bi-2212 system due to both their ion radii of different sizes and their electronic characteristics can occupy or incorporate interstitial sites in its crystal structure, meaning major changes in unit cell constants [29]. However, it is distinctly observed in Table 1 that unit cell parameters of all the samples are within their ideal values. This clearly suggests that both Na and nano-sized Sn have not entered into the Bi-2212 lattices.

On the other hand, while some ideal peak positions of the Bi-2212 phase are seen at $2\theta \approx 13.45°, 20.182°, 20.763°$, they have disappeared in sample C, showing its lower superconductivity properties. Moreover, we have observed from the XRD analysis that some major impurity phases with $CaBi_2O_4$ seen at $2\theta \approx 41.78°, 43.02°$ for sample A disappear in sample B. In addition, the peak intensities of $CaBi_2O_4$ phase seen at $2\theta \approx 52.76°, 53.73°$ in sample A decrease in sample B, meaning that the doping of SnO_2 at low amounts (x = 0.05) into the system contributes to the enhancement of the Bi-2212 phase.

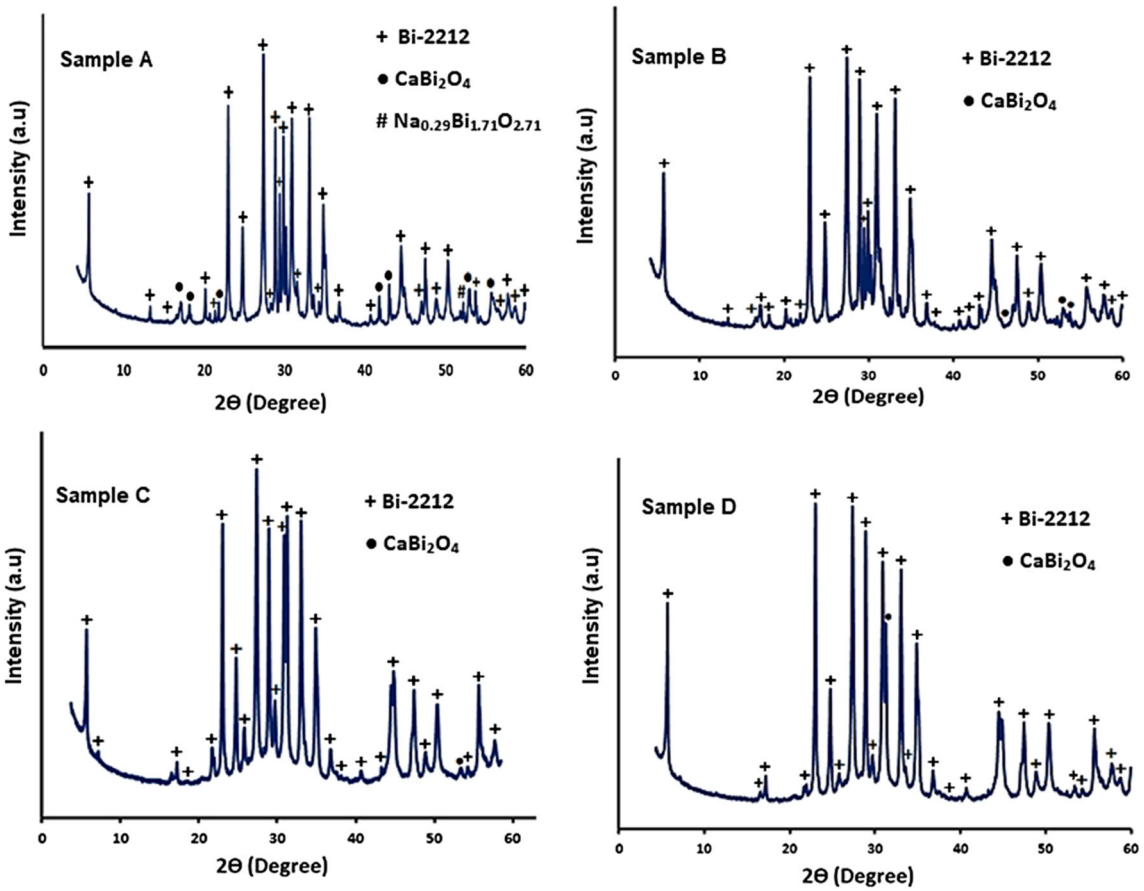

Fig. 1 XRD patterns of the A, B, C, and D samples. The symbols indicate the different phases. + Bi-2212.● Bi_2CaO_4. # $Na_{0.29}Bi_{1.71}O_{2.71}$

The SEM micrographs of the all samples are shown in Figure 2a and d. The formation of large plate-like grains seen in all the samples are associated with the characteristic of the Bi-2212 phase, indicating that the presence of Na in the system positively affects the formation and stability of the Bi-2212 phase, as expected. It is well known that the main reason for low J_c values in the ceramic superconductor results from important parameters such as the weak links between grains, high porosity, and secondary phases settled down between grain boundaries. In order to reach higher J_c values, it is necessary to have better grain orientations with larger grain sizes, implying high crystallinity. On the other hand, the parameters such as the number of pinning centers, the dispersion of SnO_2 nanoparticles, and the presence of voids inside intragrain structures can also change the transport J_c values of samples quite effectively even if all the samples have the similar granular morphology due to large grain sizes as seen in Fig. 2.

Table 1 Lattice parameters and resistivity measurement results for the samples

Samples	a (Å)	b (Å)	c (Å)	T_c^{onset} (K)	T_c^{offset} (K)
A	3.8247	3.8247	30.9014	89.08	61.4
B	3.8260	3.8260	30.8909	84.6	66.3
C	3.8314	3.8314	30.8750	82.8	35.8
D	3.8305	3.8305	30.8805	92.6	50.2

In fact, the flux pinning capability of the type II superconductors can also be increased by the enhanced grain boundary pinning as well as the creation of artificial pinning centers [30, 31]. In this sense, the behavior of nano-sized SnO_2 particles placed between the grains is also quite important. Otherwise, agglomerated SnO_2 particles can cause significant damage to the texture degree of the grains, resulting the very low J_c values.

Figure 3 shows the temperature dependence of electrical resistivity for all the samples. It is well known that as T_c (onset) is related to the degree of transition within grains as well as formation of high temperature phases, T_c (offset) reflects superconducting coupling between grains [32, 33]. The values of T_c (onset) transition temperature of A, B, C, and D samples are found for about 89.08 K, 84.6 K, 82.8 K, and 92.6 K, respectively. The result of the T_c (onset) values is in accordance with both XRD and SEM observations with the formation of large grain structure and the presence of Bi-2212 phases at high rates. However, T_c (offset) shows significant decreases for SnO_2-doped samples ($x > 0.05$), indicating the low intergrain connectivity. On the other hand, the lowest

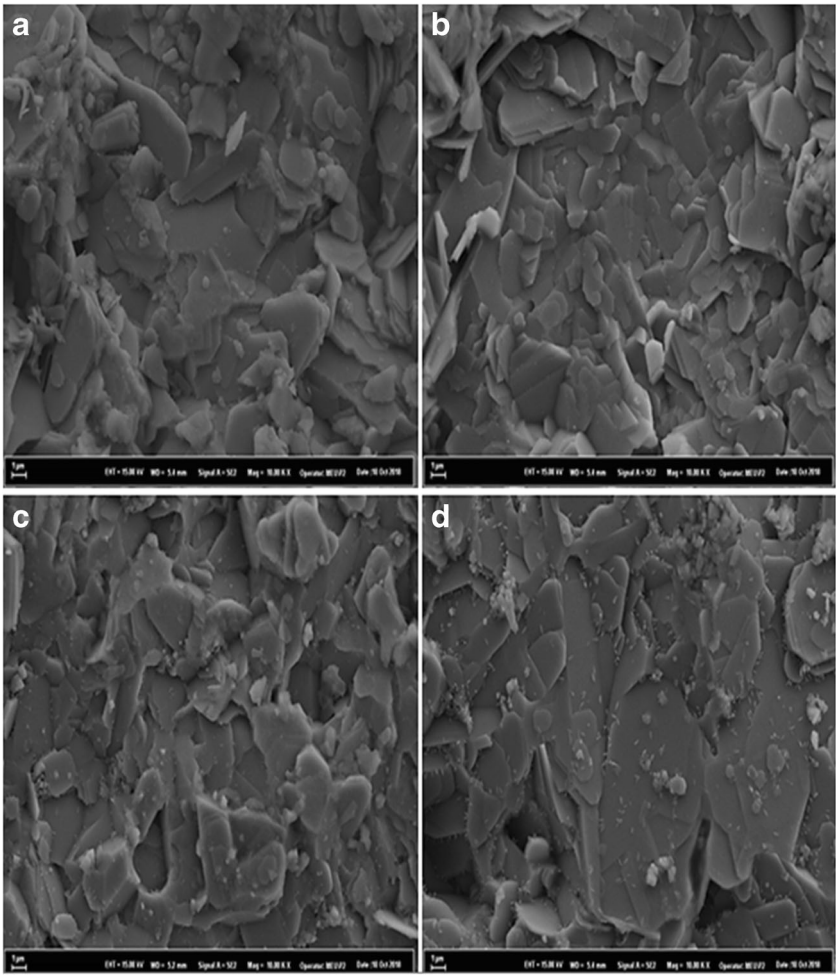

Fig. 2 SEM micrographs obtained in the surfaces of **a** A, **b** B, **c** C, and **d** D samples

transition temperature width (ΔT_c) belongs to sample B, meaning better connectivity between grains as well as its high phase purity. Clearly, similar results can be seen in other studies in the literature, which shows that the doping of nano-sized SnO_2 at high contents into the BSCCO system can cause excessive damage on superconductivity transition temperatures (T_c) due to the effect of its weak pair-breaking [34, 35]. Moreover, the hole-carrier concentrations per Cu ion (p) can be easily calculated by the Presland equation from the T_c (offset) values of the samples [36]. It can be clearly seen from Table 1 that the offset critical temperature ($T_{c,offset}$) of both samples A and B are higher compared with that of the other samples, indicating that the values of p in these samples are within the ideal range of the BSCCO system [25, 37].

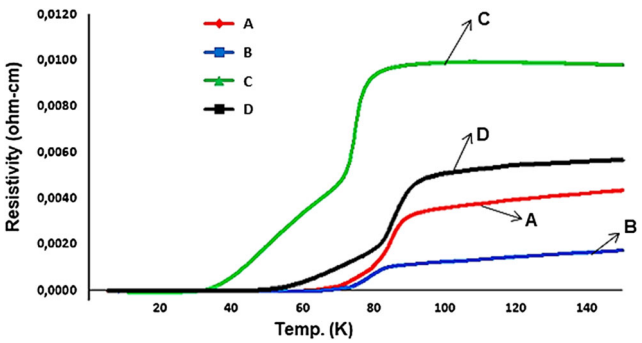

Fig. 3 Electrical resistivity as a function of temperature curves for all the samples

However, the samples including the substitutions of SnO_2 nanoparticles at high amounts ($x > 0.05$) into Bi-2212 ceramics have low $T_{c,offset}$ values, meaning a significant deterioration in the hole-carrier concentration of the Bi-2212 system.

The magnetic hysteresis cycles between applied fields of ± 2 T, for all the samples, at 15 and 25 K, are presented in Figs. 4 and 5, respectively. Enhancement of *M-H* performance in high-temperature superconductors significantly depends on many parameters such as the formation of well-crystallized superconducting grains, intergranular conductivity, and the volume fraction of the desired phases. However, the improvements in magnetization hysteresis loops at high temperatures are generally based on the enhancements of flux pinning properties in intragrain regions, implying *M-H* curves with larger areas [32, 38]. The basic diamagnetic character of type II superconductors is clearly seen in all the samples, showing that the desired superconducting phases are formed. Both

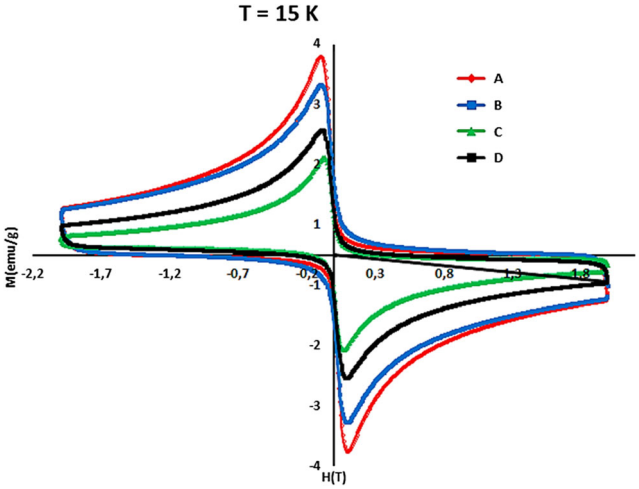

Fig. 4 Magnetization hysteresis curves for all the samples measured at 15 K and ± 2 T external applied magnetic field.

sample A, without SnO_2, and sample B, with SnO_2, at $x = 0.05$ content when compared with other samples exhibit large *M-H*, meaning the improvement of some parameters such as better electrical connectivity between superconducting grains, the formation of high amounts of superconducting phases, and the presence of effective pinning centers in the ideal amounts. In contrast, the samples with a doping level higher than $x = 0.05$ show a smaller diamagnetic signal, implying weak grain connections and low degree of crystallinity.

The critical current density of samples was calculated at 15 K, using Bean's model [39].

$$\mathrm{Jc} = 30\frac{\Delta M}{d}$$

where J_C is the magnetization current density in ampéres per square centimeter of a sample. $\Delta M = M_+ - M_-$ is measured in

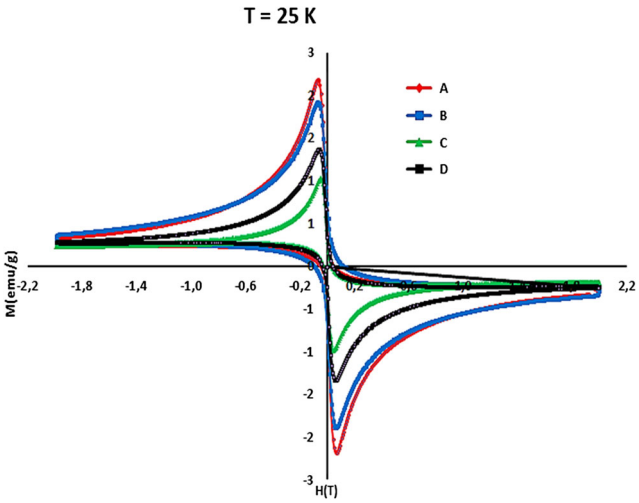

Fig. 5 Magnetization hysteresis curves for all the samples measured at 25 K and ± 2 T external applied magnetic field

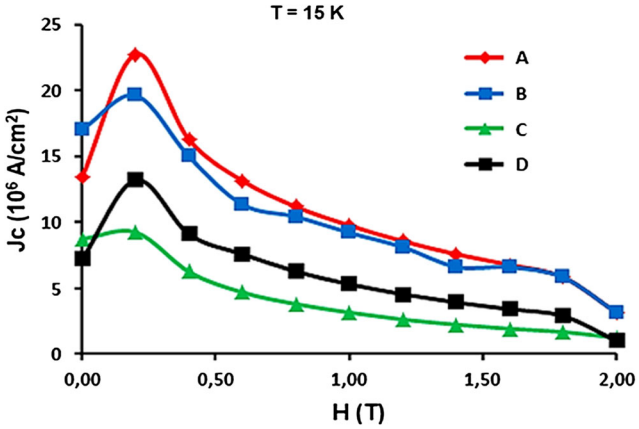

Fig. 6 Calculated critical current densities for all the samples at 15 K as a fuction of applied magnetic field

electromagnetic units per cubic centimeter, *d* is the diameter of cylindrical samples.

Figure 6 shows critical current density values depending on magnetization measurement results. In a magnetic field range of 1.6–2 T, J_c values of sample B with $x = 0.05$ content of SnO_2 almost overlap with those of sample A. However, J_c of SnO_2-doped samples at high contents quickly decreases in high magnetic fields. The J_c values at 1.9 T of sample A with undoped and sample B with $x = 0.05$ SnO_2 content are 5.847×10^6 A/cm^2 and 5.839×10^6 A/cm^2, respectively. Additionally, the J_c for both samples C and D decreases drastically, which indicates that the SnO_2 doping at high amounts for the $Bi_2Sr_2Ca_1Cu_{1.75}Na_{0.25}O_y$ starting composition gives a negative effect on J_c. Phase analysis by XRD clearly shows that there is no impurity phase with SnO_2. Thus, the nano-sized SnO_2 as secondary phase can settle in intragrain and between intergrain regions, causing poor crystallinity instead of the formation of new effective pinning centers in the samples. In this work, the best results due to the improvement of T_c (offset) and high J_c values are obtained by undoped and $x = 0.05$ SnO_2-doped sample.

4 Conclusions

In this study, the effect of nano-sized SnO_2 doping on the physical, structural, and magnetic properties of Bi-2212 ceramics is investigated by $Bi_2Sr_{2-x}(SnO_2)_xCa_1Cu_{1.75}Na_{0.25}O_y$ starting composition because of the positive effect of Na doping on grain sizes of Bi-2212 ceramics. Samples are produced by the conventional solid-state reaction method in different contents (from $x = 0.00$ to $x = 0.2$). The phase formation, lattice parameters, and surface morphologies determined by both XRD and SEM measurements for all the samples indicate the presence of Bi-2212 phase with large grain structures. All the samples show metallic behavior above their T_c (onset) values, indicating that their hole concentrations in CuO_2 plane

are within the limits of the BSCCO system. On the other hand, it was also observed that the nano-sized SnO_2 doping at low amounts ($x = 0.05$) improves T_c (offset) as based on the formation of high amounts of Bi-2212 phases. Moreover, the enhancement of T_c (offset) in sample B can also depend on better grain connectivity which is achieved with the settling of SnO_2 particles between grains.

The high values of J_c in this work belong to both undoped and sample with $x = 0.05$ doped SnO_2, which is related to the ideal number of effective pinning centers as well as the better intragrain properties. The J_c value of 2.12×10^6 A/cm^2 obtained in the previous study at 10 K for $Bi_2Sr_2Ca_1Cu_{1.75}Na_{0.25}O_y$ composition has been observed to improve as 5.839×10^6 A/cm^2 at 15 K for sample including nano-sized SnO_2-doped with $x = 0.05$ content in this study.

Acknowledgments All samples have been prepared in the MEİTAM Central Laboratory in Mersin University in Turkey. Both SEM and XRD measurements have been made in the MEİTAM Central Laboratory at Mersin University. Other measurements in this study have been made in the METU Central Laboratory in Middle East Technical University in Ankara in Turkey.

Funding Information This work is supported by the BAP Research Fund of Mersin University, Mersin, Turkey, under Grant Contract No: 2018-3-TP3-3086.

References

1. Özkurt, B.: J. Mater. Sci.:Mater. Electron. **27**, 2426 (2013)
2. Uysal, E., Ozturk, A., Kutuk, S., Çelebi, S.: J. Supercond. Nov. Magn. **27**, 1997 (2014)
3. Özkurt, B.: J. Mater. Sci.:Mater. Electron. **27**, 1 (2019)
4. Che, T., Gou, Y.F., Heng, J.Z., Sun, R.X., He, D.B., Deng, Z.G.: J. Supercond. Nov. Magn. **27**, 2211 (2014)
5. Giovannelli, F., Monot-Laffez, I.: Supercond. Sci. Technol. **15**, 1193 (2002)
6. Maeda, H., Tanaka, Y., Fukutomi, M., Asano, T.: Jpn. J. Appl. Phys. **27**, L209 (1988)
7. Sözeri, H., Ghazanfari, N., Özkan, H., Kilic, A.: Supercond. Sci. Technol. **20**, 522 (2007)
8. Jiang, L., Sun, Y., Wan, X., Wang, K., Xu, G., Chen, X., Ruan, K., Du, J.: Physica C. **300**, 61 (1998)
9. Shoushtari, M.Z., Ghahfarokhi, S.M.: J. Supercond. Nov. Magn. **24**, 1505 (2011)
10. Bouaïcha, F., Mosbah, M.F., Yildiz, F., Koçbay, N.A.: IEEE Trans. Appl. Supercond. **25**, 7200605 (2015)
11. Şakiroğlu, S., Kocabaş, K.: J. Supercond. Nov. Magn. **24**, 1321 (2011)
12. Kahraman, F., Sotelo, A., Madre, M.A., Diez, J.C., Ozkurt, B., Rasekh, S.: Ceram. Int. **41**, 14924 (2015)
13. Özçelik, B., Özkurt, B., Yakıncı, M.E., Sotelo, A., Madre, M.A.: J. Supercond. Nov. Magn. **26**, 873 (2013)
14. Özkurt, B., Madre, M.A., Sotelo, A., Yakıncı, M.E., Özçelik, B.: J. Supercond. Nov. Magn. **25**, 799 (2012)
15. Özkurt, B., Madre, M.A., Sotelo, A., Yakıncı, M.E., Özçelik, B., Diez, J.: C.: J. Supercond. Novel Magn. **26**, 1093 (2013)
16. Costa, F.M., Rasekh, S., Ferreira, N.M., Sotelo, A., Diez, J.C., Madre, M.A.: J. Supercond. Nov. Magn. **26**, 943 (2013)
17. Jia, Z.Y., Tang, H., Yang, Z.Q., Xing, Y.T., Wang, Y.Z., Qiao, G.W.: Physica C. **337**, 130 (2000)
18. Guo, Y.C., Tanaka, Y., Kuroda, T., Dou, S.X., Yang, Z.Q.: Physica C. **311**, 65 (1999)
19. Agranovski, I.E., Ilyusheckin, A.Y., Altman, I.S., Bostrom, T.E., Choi, M.: Physica C. **434**, 115 (2006)
20. Zhao, B., Wan, X., Song, W., Sun, Y., Du, J.: Physica C. **337**, 138 (2000)
21. Abou-Aly, A.I., Abdel Gawad, M.M.H., Awad, R., G-Eldeen, I.: J. Supercond. Nov. Magn. **24**, 2077 (2011)
22. Yavuz, Ş., Bilgili, Ö., Kocabaş, K.: J. Mater. Sci.:Mater. Electron. **27**, 4526 (2016)
23. Agail, A., Abd-Shukor, R.: J. Solid State Sci. Tech**. 22**, 1 (2014)
24. Sykorova, L.D., Smrckova, O., Jakes, V.: Phys. Status Solidi C. **1**, 1952 (2004)
25. Bilgili, O., Selamet, Y., Kocabaş, K.: J. Supercond.Nov.Magn. **21**, 439 (2008)
26. Kawai, T., Horiuchi, T., Mitsui, K., Ogura, K., Takagi, S., Kawai, S.: Physica C. **161**, 561 (1989)
27. Özkurt, B.: J. Mater. Sci.:Mater. Electron. **25**, 3295 (2014)
28. Yıldırım, G., Bal, S., Yücel, E., Dogruer, M., Akdoğan, M., Varilci, A., Terzioğlu, C.: J. Supercond. Nov. Magn. **25**, 381 (2011)
29. Kumar, J., Ahluwalia, P.K., Kisha, H., Awana, V.P.S.: J. Supercond. Nov. Magn. **23**, 493 (2010)
30. Jiang, C.H., Kumakura, H.: Physica C. **451**, 71 (2007)
31. Moutalibi, N., M'chirgui, A.: Physica C. **469**, 95 (2009)
32. Bilgili, O., Kocabaş, K.: J. Mater. Sci. Mater. Electron. **25**, 2889 (2014)
33. Mousavi Ghahfarokhi, S.E., Zargar Shoushtari, M.: J. Supercond. Nov. Magn. **27**, 1153 (2014)
34. Özkurt, B.: J. Matter. Sci. (2019). https://doi.org/10.1007/s10854-019-01826-8
35. Barik, H.K., Ghorai, S.K., Bhattacharya, S., Kilian, D., Chaudhuri, B.K.: J. Mater. Res. **15**, 1076 (2000)
36. Presland, M.R., Tallon, J.L., Buckley, R.G., Liu, R.S., Flower, N.E.: Physica C. **176**, 95 (1991)
37. Zelati, A., Amirabadizadeh, A., Kompany, A., Salamati, H., Sonier, J.E.: J. Supercond. Nov. Magn. **27**, 2185 (2014)
38. Jan, D.B., Coulter, J.Y., Hawley, M.E., Bulaevskii, L.N., Maley, M.P., Jia, Q.X., Maranville, B.B., Hellman, F., Pan, X.Q.: Appl. Phys. Lett. **82**, 778 (2003)
39. Bean, C.P.: Phys. Rev. Lett. **8**, 250 (1962)